Equilibrium Clusters of Metal Oxides

Willem K. Kegel*

Van't Hoff Laboratory for Physical and Colloid Chemistry, Debye Research Institute, Utrecht University, Padualaan 8, 3584 CH Utrecht, The Netherlands

Received: October 15, 2003; In Final Form: January 12, 2004

A simple toy model is analyzed within the framework of multichemical equilibrium to explain the spontaneous formation of clusters of certain metal oxides (termed "polyoxometalates" in the literature) in acidified aqueous solutions. Remarkably, thermodynamically stable clusters do not always correspond to magic numbers, i.e., local minima of the (bonding) free energy as a function of size. It is shown that cluster formation in metal oxides closely resembles micelle formation in surfactant systems.

1. Introduction

Metal oxides are ubiquitous in nature and are widely used in technology: they are important building blocks for catalysts and for nanometer-sized particles.[1] In particular, molybdenum, tungsten, vanadium, and aluminum oxide spontaneously and reversibly form clusters consisting of up to 36 monomers in acidified aqueous solutions.[2,3] Several species containing different numbers of metal-oxide monomers, with various degrees of protonation, have been detected or proposed.[4] In general, increasing proton and monomer concentrations cause increasing cluster sizes, but the sizes are different for each metal oxide. Remarkably, tungsten and molybdenum oxide are chemically almost identical but produce different cluster sizes.[4] A typical cluster is shown in Figure 1. It can be seen in this figure that a cluster mainly consists of octahedrally shaped monomers that are linked at their vertexes. These links are (reversible) chemical bonds: the vertexes linked in the clusters share an oxygen atom. Bonds form between two metal-oxide monomers when two protons combine with an oxygen atom at a vertex to produce water; see eq 1.

This paper is organized as follows. First, clustering of monomers is analyzed thermodynamically, leading to an expression for the fraction of clusters of any size q. Subsequently, within the framework of multichemical equilibrium, a simple toy model is analyzed: instead of octahedrally shaped monomers in space (see Figure 1), triangles in a plane are considered. It is shown that the qualitative behavior of metal-oxide clusters as seen in experiments is well described by this model. It is therefore concluded that chemical bonding under the constraints of geometry determines the thermodynamic stability of metal-oxide clusters. The clusters can be regarded as multiple state micelles and need not correspond to magic numbers, i.e., local minima of the (bonding) free energy as a function of size.

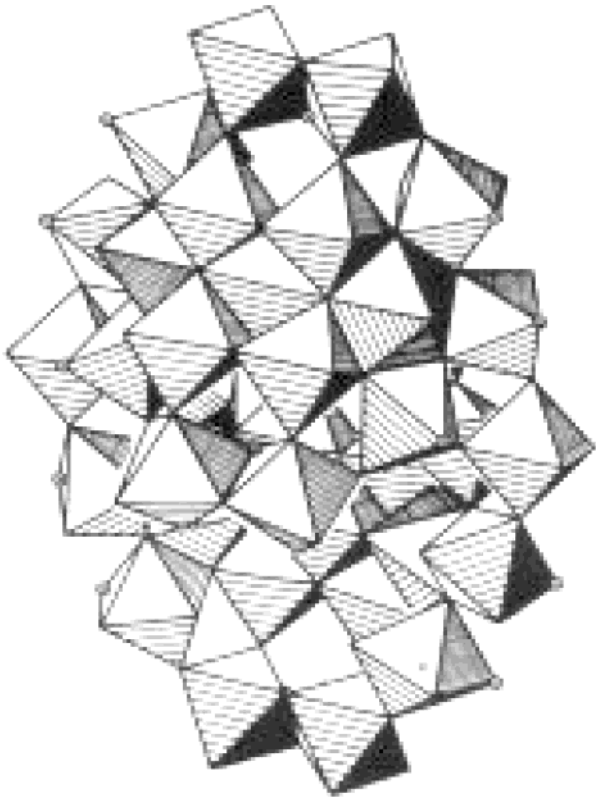

Figure 1. Typical metal-oxide polymer, in this case $Mo_{36}O_{108}$.[4] The cluster mainly consists of octahedrally shaped monomers in which the metal is located in the center of the octahedra. The vertexes of the octahedra are oxygen atoms or (valance) electron pairs. Bonds between the monomers are localized at the vertexes of the metal-oxide monomers: shared vertexes indicate bonds.

2. Multichemical Equilibrium

Reversible clustering of a metal (M) oxide in the presence of protons can be written as the multichemical equilibrium

$$pH^+ + qMO_x \rightleftarrows M_qO_{xq-p/2} + (p/2)H_2O \qquad (1)$$

where, for simplicity, species are assumed to be unprotonated. Including protonated species is straightforward but will make the analysis less transparent; it will not change the global behavior of the system. Monomers MO_x as well as q-mers $M_qO_{xq-p/2}$ are usually charged, which has not been indicated in the above equation. Thermodynamic equilibrium implies that $\sum_i \nu_i \mu_i = 0$, where ν_i and μ_i are the stoichiometric coefficients and the chemical potentials of the component i, respectively. For $i = H^+$, $i = 1$ (monomers MO_x), and $i = q$ (q-mers $M_qO_{xq-p/2}$), the chemical potential is written as $\mu_i \approx \mu_i^0 + kT \ln c_i$. Here, μ_i^0 is the standard chemical potential and c_i the concentration of component i relative to the "standard concentration" $c^0 = 1$ M (i.e., the concentration where the

* Corresponding author. E-mail: w.k.kegel@chem.uu.nl.

10.1021/jp0371229 CCC: $27.50
Published on Web 02/18/2004

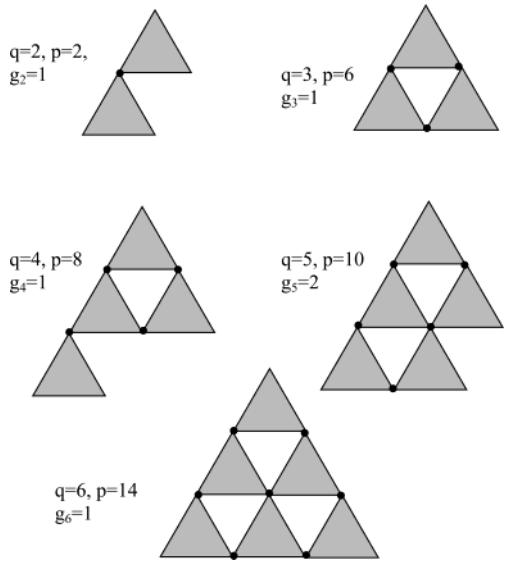

Figure 2. Toy model of polyoxometalates using packing rules as defined in the text. Starting at the top left we have $q = 2, 3, 4, 5, 6$ with $p = 2, 6, 8, 10, 14$ and $g_q = 1, 1, 1, 2, 1$. The lower row for $q = 5$ can be realized in two distinguishable ways with equal values of p as indicated in the Figure (i.e., the triangle in the lower middle row may be shifted one position to the right without changing the number of bonds), hence $g_5 = 2$.

chemical potentials have the values μ_i^0). This leads to

$$c_q = K_q g_q c_{H^+}^p c_1^q \approx g_q(\kappa_p c_{H^+})^p(\kappa_q c_1)^q \qquad (2)$$

In this equation, c_q is the concentration of species of size q: it used up p protons upon formation out of q monomers. These species can be realized in g_q ways where g_q is the degeneracy of a species q; examples are shown later (Figure 2). The key step in eq 2 is the factorization of the equilibrium constant $K_q = \exp((q\mu_1^0 - \mu_q^0 + p(\mu_{H^+}^0 - (1/2)\mu_{H_2O}^0))/kT) \approx \kappa_p^p \kappa_q^q$. This factorization is useful, i.e., κ_p and κ_q do not depend on cluster size, if the bond free energy change is at least several times the thermal energy, kT. In that case, the free energy change due to bond formation dominates the total free energy change upon forming a cluster. The cluster chemical potentials are written as $\mu_q^0 = q\mu_{1,q}^0 - (p/2)\mu_{O,q}^0$, with $\mu_{1,q}^0$ and $\mu_{O,q}^0$ the chemical potentials of a monomer MO_x inside a q-mer with composition $(MO_x)_q$, and an oxygen atom inside such a q-mer, respectively. This leads to

$$\kappa_q = \exp[(\mu_1^0 - \mu_{1,q}^0)/kT] = e^{-\Delta\mu_q} \qquad (3a)$$

$$\kappa_p = \exp\left[\left(\mu_{H^+}^0 + \frac{1}{2}\mu_{O,q}^0 - \frac{1}{2}\mu_{H_2O}^0\right)/kT\right] = e^{-\Delta\mu_p} \qquad (3b)$$

Note that the subscript q in $\mu_{O,q}^0$ is to distinguish it from oxygen in water; it does not imply that it depends on q. Thus, the factorization of the equilibrium constant in eq 2 implies that two thermodynamic forces drive the formation of equilibrium clusters: (1) $\Delta\mu_q = (\mu_{1,q}^0 - \mu_1^0)/kT$ being the reversible work of squeezing together q monomers of composition MO_x (in units of kT per monomer); this contribution is expected to be larger than zero and (2) $\Delta\mu_p = ((1/2)\mu_{H_2O}^0 - \mu_{H^+}^0 - (1/2)\mu_{O,q}^0)/kT$, the free energy change per proton due to condensation with $(p/2)$ oxygen atoms from the cluster into water, thereby forming bonds in the cluster. The latter contribution (again in units of kT) is expected to be negative and of the order 10 in magnitude, as

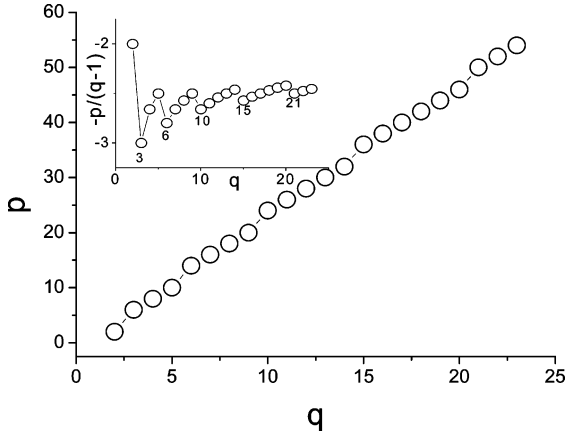

Figure 3. Number of protons, p, required to form species of size q, according to the rules depicted in Figure 2 and explained in the text. Note that p equals twice the number of bonds. The inset shows a measure of the average bond energy density, $-p/(q-1)$; local minima appear at the values of q corresponding to the magic numbers $q^* \in \{3, 6, 10, 15, ...\}$. Different geometrical rules or constraints give rise to different bond number landscapes (not shown).

estimated from measured equilibrium constants reported in ref 4. This figure is comparable to the molecular free energy change connected to micelle formation;[5] it will be shown later that this is not the only analogy with micelles. The concentrations of all q-mers may be calculated by solving eq 2 for c_1 using mass conservation, i.e., the total concentration of MO_x in the system $c = \sum_q q c_q$. This requires the numbers p and g for every q. These numbers may in principle be obtained by minimizing the free energies of all q-mers with $q \in \{2, 3, 4, ...\}$. Here, this procedure is carried out using a toy model that reflects the global features of polyoxometalates and related species.

3. Toy Model

The toy model, depicted in Figure 2, consists of triangles that contain the metal (located, e.g., at their centers). The vertexes are the oxygen atoms. Two vertexes may stick at the expense of two protons, so that the value of p is twice the number of bonds in a q-mer. A third vertex might be added, but will not stick. The stable configuration of triangles (i.e., the one that defines p, g) is the one that maximizes the number of bonds under geometrical constraints. These constraints are chosen to be (1) triangles may only be packed into a larger triangle starting with a single one at the (virtual) top; (2) rows should be filled up with triangles in order to proceed to the next row. These constraints reflect the (a priori unknown) constraints that nature imposes. In fact, many geometrical rules will lead to qualitatively similar results as the ones to be presented here, but the sizes of the stable clusters differ. Real metal-oxide monomers have octahedral or tetrahedral shapes and may even be hydrated, so that finding the rules that define real clusters is entirely nontrivial. However, the analysis of the toy model is straightforward. Figure 2 shows the situation up to $q = 6$. Any number q where a row is completely filled with triangles corresponds to a magic number, q^*: for any q^*, the number of bonds (indicated as dots) per monomer is larger than that of species $(q^* - 1)$. These magic numbers, $q^* \in \{3, 6, 10, 15, 21, 28, ...\}$ have a single complexion (no degeneration) or $g_{q^*} = 1$. The number g_q increases with unity between two magic numbers for every $q = q^* + 2n$ with $n \in \{1, 2, 3, ...\}$ or becomes 1 again if the next q is a magic number. The number of protons, $p(q)$, consumed upon forming a cluster of size q, is twice the number of bonds in a cluster. For the number of bonds

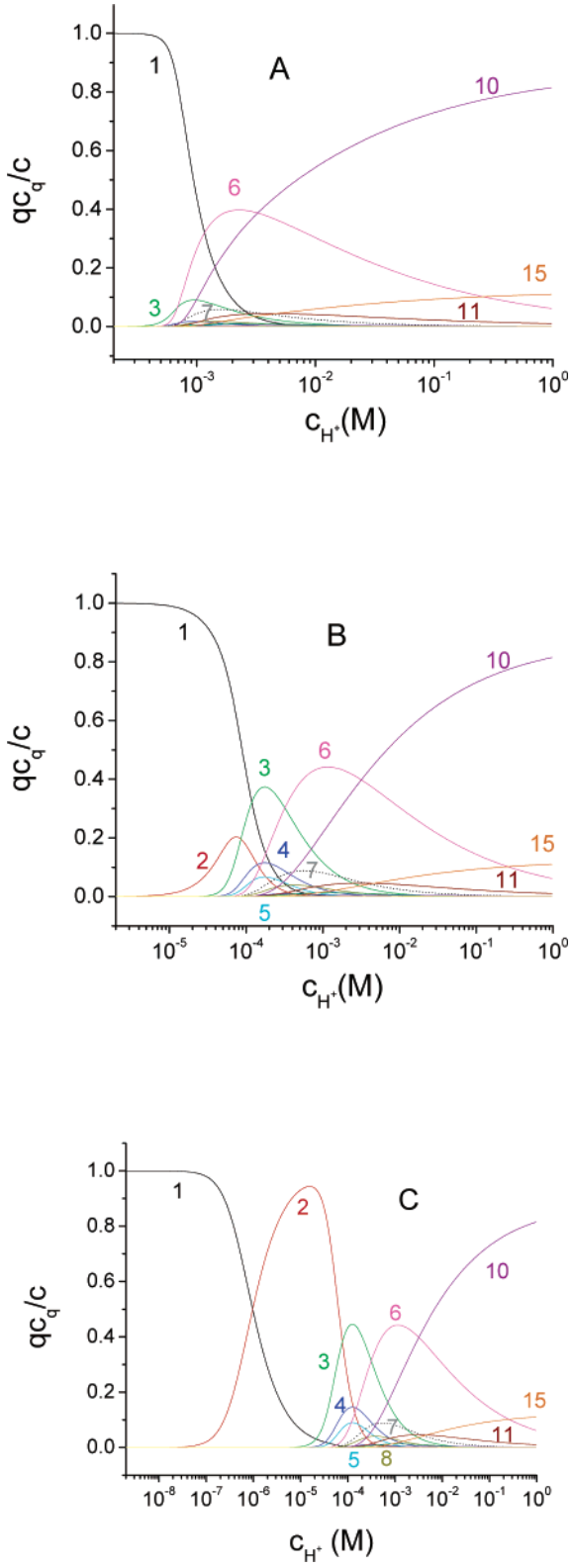

Figure 4. Fraction of species of size q (indicated in the figure) as a function of the proton concentration. These fractions qc_q/c were calculated by numerically solving eq 2 using mass conservation and a total concentration of monomers $c = 0.1$ M and (see eq 3) $\Delta\mu_p = -10$, $\Delta\mu_q = 5$ (Figure 4A), $\Delta\mu_q = 0$ (Figure 4B), $\Delta\mu_q = -5$ (Figure 4C). This polynomial in c_1 converges for large q; the concentration of all species with $q > 15$ always is less than a few percent of the total monomer concentration. In real systems, small protonated species appear at high H^+ concentrations; these species are not considered here.

we have $(1/2)p(q = 2) = 1$ and $(1/2)p(q + 1) = (1/2)p(q) + 1$ if $q + 1 \notin q^*$, while $(1/2)p(q + 1) = (1/2)p(q) + 2$ if $q + 1 \in$

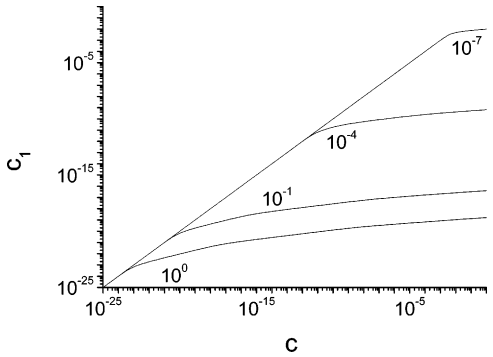

Figure 5. Concentration of free monomers, c_1, as a function of the total monomer concentration, c, at several values of the proton concentration indicated in the figure. Curves are plots of the function $c = \sum_q qc_q$ using $\Delta\mu_p = -20$ and $\Delta\mu_q = 5$ in eqs 2 and 3. The crossovers from c_1 rising linearly with c to almost constant values indicate cluster formation analogous to the formation of micelles in surfactant solutions. The values of the critical cluster concentrations, c_1^* (see text) can be checked by noting that $q' = 3$ (as in Figure 4A).

q^*. These rules lead to the bumpy landscape as depicted in Figure 3. Also shown in this figure is a measure of the "bond energy density" $-p/(q - 1)$. This quantity is plotted in (the inset of) Figure 3; the minima clearly correspond to magic numbers.

4. Results and Discussion

Figure 4 shows the fraction of species q as a function of proton concentration at a single value of $\Delta\mu_p = -10$ and different values of $\Delta\mu_q$. The same trends are observed upon variation of the total monomer concentration, c, at constant proton concentrations (not shown). These trends are the following: (1) only a relatively small number of species are observed in significant concentrations; (2) the fractions of the smallest species go through maxima; and (3) larger species are observed upon increasing proton and total monomer concentrations. These trends are in agreement with experimentally observed behavior of polyoxometalates.[2−4] This agreement verifies the widely shared notion that both geometry and chemical bonding play roles in the stability of the clusters. However, not only magic numbers appear but also small but significant fractions of species with $q \neq q^*$, depending on the proton concentration. Thus, in real systems, the full "bond number landscape" (see Figure 3) should be taken into account; it is not sufficient to look for magic numbers. It can also be seen in Figure 4 that repulsive monomer interactions, $\Delta\mu_q > 0$, suppress the formation of small species, whereas decreasing $\Delta\mu_q$ leads to a significant increase of small clusters. This increase of small clusters upon decreasing $\Delta\mu_q$ may explain why in case of molybdenum and tungsten oxide, only (unprotonated) species with $q \geq 6$ have been observed while in case of aluminum oxide, significant fractions of dimers ($q = 2$) appear.[2] It is quite feasible that the relatively large hydration layer of aluminum oxide causes a smaller or even negative value of $\Delta\mu_q$, thereby stabilizing small clusters. The present analysis also suggests that the differences in cluster sizes between the chemically similar tungsten and molybdenum oxide must be due to different packing rules of the octahedrally shaped monomers. These different rules may in turn be caused by a combination of subtle effects, including again hydration.

It is worth noting that the above behavior resembles micelle formation. The concentration of monomers at which the first species of size $q' > 1$ appear follows from eq 2 and is given by $c_1^* \approx [g_{q'}\kappa_q^{q'}(\kappa_p c_{H^+})^p]^{-1/(q'-1)}$. This concentration reduces to the

critical micelle concentration derived by Debye[6] if $\kappa_p c_{H^+} = g_{q'} = 1$. In the situation described here, the "critical cluster concentration", c_1^*, sensitively depends on proton concentration. Figure 5 shows that, at c_1^*, a crossover occurs from c_1 increasing linearly with c, to c_1 being more or less constant; this behavior is indeed fully comparable to micelle formation. Note that for micelles, cluster distributions are centered around $q' \approx 50-80$ [5] depending on the type of surfactant(s) used.

Finally, a combination of geometry and multichemical equilibrium has proved quite successful in explaining the stability of virus capsids that consist of (many) coat protein building blocks, see ref 7 and, more recently.[8] Thus, it seems that viruses, metal-oxide clusters, and surfactant micelles can all be described by similar concepts. Indeed, under appropriate conditions, intricate structures comparable to virus capsids form in certain mixtures of metal oxides, see ref 9. Incorporating the basic geometry of these systems into a model remains an interesting challenge ahead.

Acknowledgment. I thank Roel Dullens, Paul van der Schoot, and Ivana Validzic for discussions and Martijn Oversteegen for comments on the manuscript.

References and Notes

(1) Müller, A.; Krickemeyer, E.; Dillinger, S.; Bogge, H.; Proust, A.; Plass, W.;q Rohlfing, R. *Naturwissenschaften* **1993**, *80*, 560−564.
(2) Baes, C. F.; Mesmer, R. E. *The Hydrolysis of Cations*; Wiley: New York, 1976.
(3) Tytko, K.-H.; Glemser, O. *Adv. Inorg. Chem. Radiochem.* **1976**, *19*, 239−315.
(4) Tytko, K. H. *Gmelin Handbook of Inorganic Chemistry: Molybdenum*, 8th ed.; Springer: Berlin, 1987; Vol. B 3a.
(5) Israelachvili, J. *Intermolecular & Surface Forces*, 2nd ed.; Academic Press: San Diego, 1992.
(6) Debye, P. J. W. *Ann. NY Acad. Sci*. **1949**, *51*, 575−592.
(7) Zlotnick, A. *J. Mol. Biol.* **1994**, *241*, 59.
(8) Bruinsma, R. F.; Gelbart, W. M.; Raguerra, D.; Rudnick, J.; Zandi, R. *Phys. Rev. Lett.* **2003**, *90*, 248101.
(9) Müller, A.; Kögerler, P.; Bögge, H. *Structure Bonding* **2000**, *96*, 203.